

LETTER

Target Classification Using Features Based on Fractional Fourier Transform

Jongwon SEOK^{†a)} and Keunsung BAE^{††b)}, Members

SUMMARY This letter describe target classification from the synthesized active sonar returns from targets. A fractional Fourier transform is applied to the sonar returns to extract shape variation in the fractional Fourier domain depending on the highlight points and aspects of the target. With the proposed features, four different targets are classified using two neural network classifiers.

key words: target, recognition, active sonar, pattern recognition, LFM, highlight model, fractional Fourier transform

1. Introduction

Various approaches to process active sonar signals are under study, but there are many problems to be considered. The sonar signals are distorted by the underwater environment, and the temporal and spectral characteristics of active sonar signals change in accordance with the aspect of the target even though they come from the same one. In addition, since it is difficult to collect real data for research, most researchers focus on experimentally generated data such as sonar returns from submerged elastic cylindrical shaped targets in a water tank or lake [1]–[3]. An alternative approach is to use sonar signals synthesized for certain target condition. In that case conventional echo highlight model [4] could be used because of its simplicity.

This letter presents a method for classifying the target using the synthesized active sonar returns. Active sonar returns from targets are synthesized based on the ray tracing algorithm for 3D highlight models. To extract the features, a fractional Fourier transform (FrFT) is applied to sonar returns. With the FrFT-based features, four different targets are classified using two neural network classifiers. To prove the effectiveness of FrFT-based features, we compare the performance of the proposed method with conventional Fourier transform (FT) using same feature extraction method.

2. Synthesis of Active Sonar Returns

For the synthesis of active sonar returns, an underwater environment with direct reflections from the target and indirect reflections from sea level and sea bottom was assumed. Figure 1 shows the relationship between target model and source/receiver sensor on x-y coordinate. In Fig. 1, target lies in the x-axis direction and θ is the angle between target and source/receiver sensor. The depth of water was set to 300 m. The source and receiver were located at the same position in the water, i.e. monostatic mode as shown Fig. 1, and an unknown target was at 50m below sea level. We adopted the sound velocity profile to calculate the sound velocity at a certain depth of water. Four targets with different shapes were modeled using a 3D highlight model, and active sonar returns from each target depending on the target aspects were synthesized using a tracing method considering the sound velocity profile [5].

Figure 2 shows highlighted models of the four targets designed for the synthesis of sonar returns. All the targets have several highlights lying mainly in the horizontal line. Each highlight is assumed to reflect the acoustic wave in all directions. All echo components can be considered a summation of an individual echo from certain equivalent scattering points. The underwater target can be characterized by the highlights distributed within a spatial target structure. Underwater acoustic wave is then propagated over being attenuated and bent by sound velocity. We can obtain the synthesized signal by summing traced signals from each highlight at the receiver position.

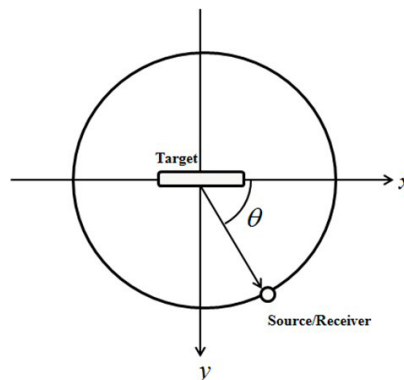


Fig. 1 Relationship between target model and source/receiver on x-y coordinate.

Manuscript received January 6, 2014.

Manuscript revised May 22, 2014.

[†]The author is with the Department of Information and Communication, Changwon National University, Sarimdong, Uichang-gu, 641-773, Changwon, Korea.

^{††}The author is with the School of Electronics, Kyungpook National University, 1370 Sankyukdong, Bukgu, 702-701, Daegu, Korea.

a) E-mail: jwseok@chagwon.ac.kr

b) E-mail: ksbae@ee.knu.ac.kr

DOI: 10.1587/transinf.2014EDL8003

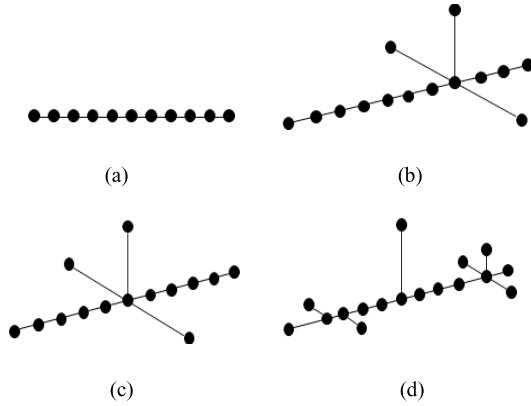


Fig. 2 3D highlight models of targets for synthesis of active sonar signals. (a) Type 1 (b) Type 2 (c) Type 3 (d) Type 4.

3. Feature Extraction Based on Fractional Fourier Transform

3.1 Fractional Fourier Transform

Namias first introduced fractional Fourier Transform in the field of quantum mechanics to solve some classes of differential equations in 1980 [6]. Later, Ozaktas introduced an algorithm for digital calculation of FrFT [7]. Since then, a number of applications of FrFT have been developed [8]–[10].

The FrFT is a generalization of the conventional Fourier transform and has a history in mathematical physics and digital signal processing. Basically, it is considered a one-parameter subclass of the linear canonical transforms. This parameter is called the fractional order of the transform, which is denoted by α . The FrFT relies on a parameter α and can be interpreted as a rotation by an angle in the time-frequency plane. If $\alpha = 0$, the FrFT corresponds to an identity operator, and when $\alpha = 1$, it becomes a Fourier transform. The α^{th} order FrFT of a signal $s(t)$ can be obtained by

$$F_{\alpha}(u) = \sqrt{1 - i \cot\left(\frac{\alpha\pi}{2}\right)} \int_{-\infty}^{\infty} \exp\left[i\pi\left(\cot\left(\frac{\alpha\pi}{2}\right)u^2 - 2 \operatorname{csc}\left(\frac{\alpha\pi}{2}\right)uv + \cot\left(\frac{\alpha\pi}{2}\right)v^2\right)\right] s(v)dv \quad (1)$$

where u and v define the axes of the fractional domain.

The potential of FrFT lies in its ability of FrFT to process chirp like signals better than the conventional Fourier transform. If the frequency of a signal varies with time such as LFM signal, we can obtain the optimal transform result with an optimal transform order α_{opt} which is maximally compressed with smallest bandwidth [8]. The optimal transform order α_{opt} can be defined as

$$\alpha_{opt} = -\frac{2}{\pi} \tan^{-1}\left(\frac{f_s^2/N}{2a}\right) \quad (2)$$

where a is the chirp rate, f_s is the sampling frequency, and N is the total number of time samples.

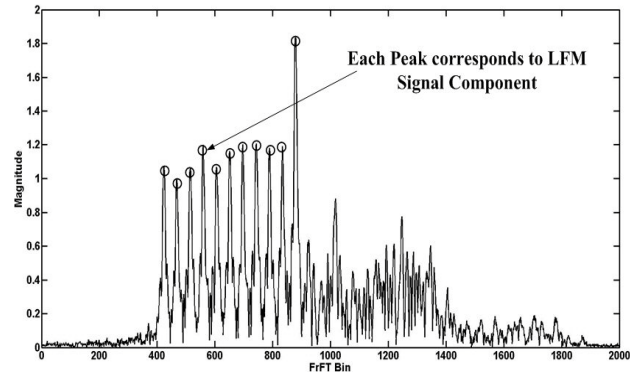


Fig. 3 Result of the FrFT of the target Type 1 at 0° .

3.2 Feature Extraction Process

A simple LFM signal at the transmitter can be defined as

$$s(t) = A \cos\left[2\pi t\left(f_c + \frac{B}{2}t\right)\right] \quad (3)$$

where B is the bandwidth and f_c is the center frequency.

The signal received from the highlight model can be expressed as

$$r(t) = \sum_{m=1}^N \left\{ A_m \cos\left[(t - \tau_m)\left(f_c + \frac{B}{2}(t - \tau_m)\right) + \varphi_m\right] \right\} \quad (4)$$

where N is the number of highlight points, A_m is the amplitude, τ_m is the time delay, and φ_m is the phase component of scattered signals from each highlight point, respectively.

An active sonar return is obtained by summing multiple time-overlapped LFM signals reflected from the highlighted points of a target. The FrFT of order, α_{opt} , was performed on the signal received from the highlight model. The application of the FrFT with an optimal order to the multiple time-overlapped LFM signals compresses the signals maximally in the FrFT domain, where multiple LFM signals are represented by multiple peaks [11]. Figure 3 shows the result of the FrFT of the target Type 1 at aspect angle of 0° . As shown in Fig. 3, backscattered multiple LFM signals from each highlight points of the target Type 1 are represented by multiple peaks.

Time delays, which vary depending on the aspect angle of the target, determine the distances among the peaks. Multiple peak positions in the FrFT domain were determined by different time delays from each highlight point to the receiver. Therefore, the main bandwidth of the signal received in the FrFT domain also depends on the time delays of multiple LFM signals.

The main idea to classify the target is reflecting the shape variation of the peak positions depending on the highlight points of the target. The best way to achieve accurate shape variation is the use of entire FrFT coefficients as a feature vector. However, the entire FrFT coefficients contain too much redundant and irrelevant information, this can lead

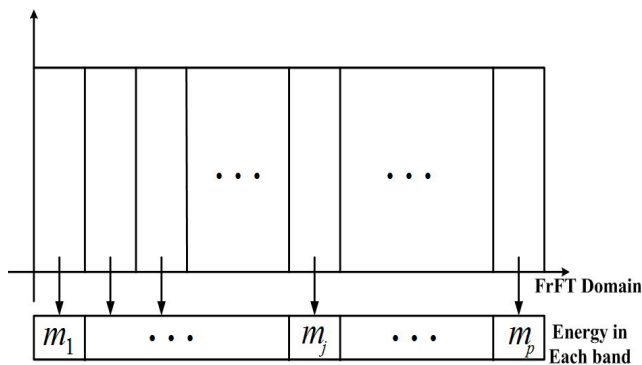


Fig. 4 Feature extraction process in FrFT domain.

to decrease of discrimination capability. Therefore, to reflect shape variation properly, the feature vector is obtained by dividing the FrFT domain into 100 equal bands and calculating the energy for each band. This process produces 100 FrFT based features which reflect the characteristics of shape change adequately and possess discrimination capability. Figure 4 illustrates the feature extraction process.

4. Experimental Results

In the synthesis of active sonar signals, the sampling frequency and LFM pulse duration was set to 31.25 kHz and 50ms, respectively. The center frequency and bandwidth of the LFM signal were 7 kHz, and 400 Hz, respectively. The signals synthesized by summing the signals traced from each highlight model depending on aspect angle of the target were then obtained. In this study, 1440 active sonar returns were generated from four highlight models by varying its aspect from 0 to 359° in 1° increments.

Figure 5 and 6 show the features extracted from four different targets at aspect angle of 45° in the FrFT and conventional FT domain through the feature extraction process of Fig. 4, respectively. Features extracted from four different targets have different shapes in FrFT domain depending on target type. On the other hand, features extracted in FT domain show relatively similar shapes, compare to the features extracted in FrFT domain in Fig. 5.

To validate the effectiveness of the proposed method, the classification test was carried out. In this experiment, backpropagation neural network (BPNN) [12] and probabilistic neural network (PNN) [13] were selected. BPNN and PNN have been employed efficiently as pattern classifiers in numerous applications.

PNN has 3 layers of neurons. The input layer contains 100 neurons: one for each of the 100 input features of a feature vector. These are fan-out neurons that branch at each feature input neurons to all neurons in the hidden layer so that each hidden neuron receives the complete input feature vector. The hidden neurons are collected into groups: one group for each of the four target classes. In case of BPNN, we used 100-24-4 structure, with 100 input neurons, 24 hidden-layer neurons, and four outputs. The stopping

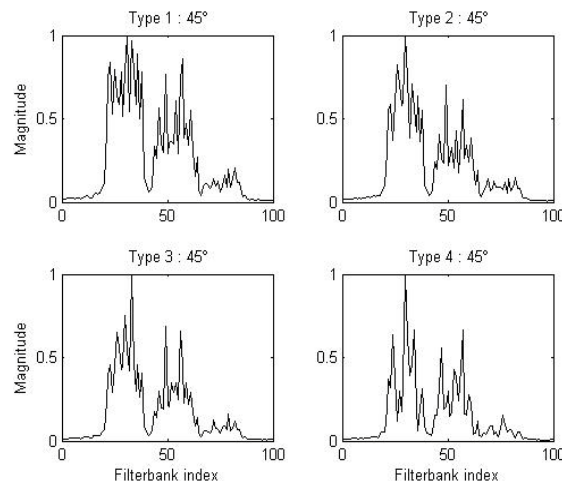


Fig. 5 Features extracted from four different targets at aspect angle of 45° in the FrFT domain.

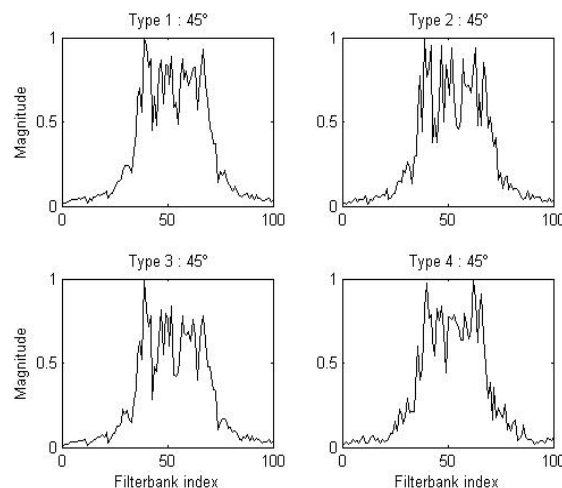


Fig. 6 Features extracted from four different targets at aspect angle of 45° in the FT domain.

criterion used is as follows: the training is stopped either when the average error is reduced to 0.001 or if a maximum of 10,000 epochs is reached.

Among a total 1440 data set, 360 samples were used to train the neural networks and the remaining 1080 samples were used to test the classification performance. We also compared the performance of proposed method with conventional FT using same feature extraction method. Features in the FT domain were obtained by dividing the Fourier spectrum into 100 equal bands and calculating the energy for each band.

Table 1 lists the experimental results. PNN shows slightly better recognition rate than BPNN. Because of the asymmetric highlight model structure, Type 2 and 4 showed slightly lower recognition rates than Type 1 and 3. However, there were no distinct differences in recognition rate depending on the highlight types and aspect angles.

In conventional FT domain, individual LFM signals overlap with same bandwidth and center frequency not

Table 1 Result of recognition experiment.

	BPNN		PNN	
	FT	FrFT	FT	FrFT
Type 1	68.98%	89.17%	69.44%	90.56%
Type 2	67.69%	86.67%	68.06%	87.69%
Type 3	66.67%	87.78%	67.31%	88.80%
Type 4	67.87%	86.67%	68.80%	87.96%
Total	67.80%	87.57%	68.40%	88.75%

reflecting time delay information from each highlight point to the receiver. Therefore, features extracted from each targets in FT domain show similar shapes depending on target type as shown in Fig. 6. On the other hands, features extracted from each targets in FrFT domain reflect the time delay information. And, time information changes spectral shape in FrFT domain depending on target type. This is the main advantage of FrFT-based features and directly related to recognition performance. From Table 1 it is clear that proposed FrFT-based features outperforms conventional FT-based features in all cases.

5. Conclusion

This letter has described a feature extraction, using FrFT-based features and synthesized active sonar returns, for target classification. A fractional Fourier transform is applied to the sonar returns to extract the shape variation in FrFT domain which depends on the highlight points and aspects of the target. With the FrFT-based features, four different targets were classified using two neural network classifiers. Using the FrFT-based features, we could obtain a better recognition rate, approximately 20%, than conventional FT-based features. Though the synthesized active sonar signals are in very limited conditions because we assumed very simple target models and environment, simulation results have shown that the given target classification scheme using FrFT-based features is appropriate for active sonar target classification.

Acknowledgments

This work was supported by Defence Acquisition Program

Administration and Agency of Defence Development under the contract UD130007DD.

References

- [1] A. Pezeshki, M.R. Azimi-Sadjadi, and L.L. Scharf, "Undersea target classification using canonical correlation analysis," *IEEE J. Ocean. Eng.*, vol.32, no.4, pp.948–955, Oct. 2007.
- [2] M.R. Robinson, M.R. Azimi-Sadjadi, and J. Salazar, "Multi-aspect target discrimination using hidden Markov models and neural networks," *IEEE Trans. Neural Netw.*, vol.16, no.2, pp.447–459, March 2005.
- [3] M.R. Azimi-Sadjadi, D. Yao, A.A. Jamshidi, and G.J. Dobeck, "Underwater target classification in changing environments using an adaptive feature mapping," *IEEE Trans. Neural Netw.*, vol.13, no.5, pp.1099–1111, Sept. 2002.
- [4] B. Kim, H. Lee, and M. Park, "A study on highlight distribution for underwater simulated target," *Proc. ISIE 2001*, vol.3, pp.1988–1992, 2001.
- [5] A. Michael, *Principles of sonar performance modeling*, Springer-Verlag, Berlin, 2010.
- [6] V. Namias, "The fractional order Fourier transform and its application to quantum mechanics," *IMA J. Appl. Math.*, vol.25, no.3, pp.241–265, March 1980.
- [7] H. Ozaktas, O. Arikan, M. Kutay, and G. Bozdogt, "Digital computation of the fractional Fourier transform," *IEEE Trans. Signal Process.*, vol.44, no.9, pp.2141–2150, 1996.
- [8] C. Capus and K. Brown, "Short-time fractional Fourier methods for the time-frequency representation of chirp signals," *J. Acoust. Soc. Am.*, vol.113, no.6, pp.3253–3263, June 2003.
- [9] A.W. Lohmann, "Image rotation, Wigner rotation, and the fractional Fourier transform," *J. Opt. Soc. Am. A*, vol.10, no.10, pp.2181–2186, Oct. 1993.
- [10] H. Ozaktas, Z. Zalevsky, and M. Kutay, *The Fractional Fourier Transform: With Applications in Optics and Signal Processing*, Wiley, New York, NY, 2001.
- [11] M. David and F. Steven, "Separation of overlapping linear frequency modulated (LFM) signals using the fractional Fourier transform," *IEEE Trans. Ultrason. Ferroelectr. Freq. Control*, vol.57, no.10, pp.2324–2333, Oct. 2010.
- [12] S. Haykin, *Neural Network*, McMillan, New York, 1994.
- [13] D.F. Specht, "Probabilistic neural network," *Neural Netw.*, vol.3, pp.109–118, 1990.